B.G. Shabalin, Dr.Sc. (Geology), Head of Department
E-mail: b_shabalin@ukr.net; https://orcid.org/0000-0002-6425-5999
K.K. Yaroshenko, PhD (Engineering), Researcher
E-mail: igns.yaroshenko@gmail.com; https://orcid.org/0000-0002-7180-4642
O.M. Lavrynenko, Dr.Sc. (Chemistry), Leading Researcher
E-mail: alena.lavrynenko@gmail.com; https://orcid.org/0000-0002-5271-2048
N.B. Mitsiuk, Junior Researcher
E-mail: nmitsiuk@gmail.com; https://orcid.org/0000-0003-3875-007X
State Institution "The Institute of Environmental Geochemistry
of National Academy of Sciences of Ukraine"
34-a, Acad. Palladin Ave., Kyiv, Ukraine, 03142

MINERAL COMPOSITION AND ADSORPTION CAPACITY OF PRECIPITATES FORMED DURING OZONATION OF RADIOACTIVELY CONTAMINATED WATER FROM NUCLEAR POWER PLANTS TOWARDS ^{137}Cs

The mineral composition and sorption properties of precipitates formed during ozonation of a model solution simulating nuclear power plant wastewater (total mineralization 7 g/dm³, pH = 11.5, T = 60 °C, t = 2 hours) ^{137}Cs were studied. The precipitate is represented by finely dispersed spherical particles of metal oxides ranging in size from 20 to 30 nm, forming microaggregates and their associates of various shapes. The composition of the precipitates, along with X-ray amorphous phases, includes Fe(II)-Fe(III) layered double hydroxides (Green Rust), as well as LDH of mixed composition, in particular Fe-Co, and iron oxyhydroxides - goethite and lepidocrocite. The precipitates also contain manganese-containing phases represented by manganese (IV) hydroxide and manganese (II) carbonate with an admixture of manganese oxides, such as $Mn_2O_3 \cdot H_2O$, MnO, Mn_3O_4 (gaussmanite). In the process of ozonation, organic compounds that are part of the solutions undergo destruction, co-precipitation with other components of the solution, which is accompanied by the sorption of ^{137}Cs radionuclides on the surface of mineral particles. An increase in the concentration of Fe^{2+} and Mn^{2+} cations by 10 times (up to 50 and 100 mg/dm³, respectively) in wastewater reduces the concentration of ^{137}Cs in the initial solution by 50.5%.

Keywords: NPP wastewater, ozonation, precipitates, chemical and mineral composition, adsorption, cesium.

Introduction. Treatment of liquid radioactive waste (LRW) from Nuclear Power Plants (NPPs) is one of the most challenging tasks of the radioactive waste management [1, 24].

Ukrainian NPPs produce wastewater in the form of low salinity radiation-contaminated aqueous solutions (RCS). The total RCS salinity is 3-7 g/dm³. The wastewater treated by evaporation forming sparingly soluble salts — residues and then salt melt which is accumulated in special storage facilities in significant volumes [13].

60

ISSN 2519-2396. Mineral. Journ. (Ukraine). 2022. 44, No. 2

LRW treatment is a complicated process due to the variety of forms and physicochemical composition of the compounds containing radionuclides. The crucial radionuclides for the Ukrainian NPPs LRW are ^{134}Cs, ^{137}Cs, ^{60}Co, and ^{54}Mn. Besides radionuclides, the LRW contains corrosion products, and complexing and special detergents (surfactants). The microcomponents are in various forms, such as solvates, double and mixed complexes, singly and multi charged hydrolysis products, and colloids. As a result, there is no one universal method of the LRW decontamination and a combination of several methods should be applied in a certain order. The currently used thermal method can be supplemented by radionuclide extraction from the wastewater by adsorption and/or ion exchange.

Ozonation, as one of the environmentally safe methods of the RCS organic contaminants destruction (predominantly ethylenediaminetetraacetic and oxalic acids) and conversion of the ^{60}Co, ^{54}Mn radionuclides into an unbound form, is a constituent of a precipitation-adsorption (or oxidation-adsorption) technological process of LRW purification from radionuclides, which determines its cost-efficiency and quality [18, 25].

The organic components of RCS and LRW are oxidized by passing ozone from an ozone generator through the waste stream that was pre-filtered with a filter medium [25]. Coagulants and oxidation catalysts, for example Fe^{2+} and Mn^{2+} salts, are added to the ozonation tank to increase the efficiency of degradation of organic contaminants at high pH (8-11) owing to the Fenton process [21, 27]. During ozonation, organic substances contaminating the sorbents are destroyed, while ^{60}Co, ^{54}Mn and ^{55}Fe (activation products) are converted into the adsorbed form. A disperse phase (secondary RW) — precipitates of hydroxides, oxyhydroxides and Fe oxides, is formed, on which the activation products, ^{134}Cs, ^{137}Cs isotopes (the main dose-forming radionuclide in RCS and LRW), and ^{90}Sr co-precipitate and get adsorbed.

Considering the reduced solubility of hydroxides and increased partition coefficients of Co and Mn, absence of borate precipitation from the solutions and high efficiency of sorbents towards ^{137}Cs and ^{90}Sr radionuclides, pH of the solution during ozonation should be maintained at values ≥9. In such conditions the oxidation products are efficiently separated from the liquid phase by filtering. The optimum temperature of the solution in the ozonation process is about 60 °C [22]. The amount of the precipitate formed during ozonation depends on the composition of the solution and does not exceed one percent (from 1 to 4 g per litre of the initial solution) [22].

It is known that freshly precipitated hydroxides, oxyhydroxides and Fe oxides have increased sorption capacity [2] and more complete adsorption of cations at pH ≥ 7 [4, 6]. Alkaline cations are adsorbed on the surface of hydroxides, oxyhydroxides and oxides and are easily desorbed, while multi charged cations are adsorbed in the interlayer space of oxyhydroxides of such compounds with the possibility of formation of coordination compounds on the surface of the oxides, which results in rather slow desorption of the cations [4].

The aim of the article is definition of the mineral composition of precipitates, formed in ozonation process of Nuclear Power Plants trap waters model solutions and their sorption properties about ^{137}Cs, the main dose-forming radionuclide.

Experimental. A simulant NPP wastewater solution of the following ionic composition was prepared: Na^+ — 1593 mg/dm^3; BO_3^{3-} — 2000 mg/dm^3; K^+ — 386 mg/dm^3; Cl^- — 999 mg/dm^3; NO_3^- — 694 mg/dm^3; SO_4^{2-} — 1708 mg/dm^3; Co^{2+} — 50 mg/dm^3; Mn^{2+} — 10 mg/dm^3; Cs^+ — 50 mg/dm^3; Sr^{2+} — 50 mg/dm^3; Ca^{2+} — 5 mg/dm^3; Fe^{3+} — 5 mg/dm^3. In addition to the stable Cs isotope, a radioactive tracer ^{137}Cs isotope of the known activity was added to the solution. The ^{137}Cs activity in the solutions was determined by γ spectrometry. The ^{137}Cs activity was $3.45 \cdot 10^4$ Bq/dm^3. The total mineralization (salt content) of the solution was about 7 g/dm^3. The pH of the solution was adjusted to 11.5 with alkali (NaOH). The salt composition of the NPP simulated wastewater solution is given in Table 1. Coagulants in the form of $FeSO_4 \cdot 7H_2O$ and $MnSO_4 \cdot H_2O$ salts were added to the initial solution. The experiment was repeated with the increased concentrations of iron to 50 mg/dm^3 or manganese to 100 mg/dm^3, as well as of both salts simultaneously.
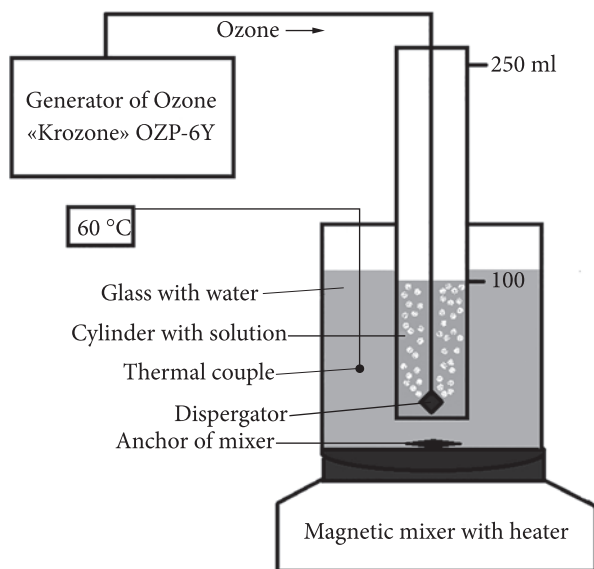
Fig. 1. Scheme of the laboratory ozonation plant

Table 1. **Salt composition
of the simulated NPP wastewater solution**

Compound	Concentration, mg/dm^3
H_3BO_3	1700
KNO_3	1000
Na_2SO_4	2000
NaCl	1450
NaOH (45%)	1450
$CoSO_4$	132
$MnSO_4 \cdot H_2O$	30.77
$Sr(NO_3)_2$	120.5
$CsNO_3$	73.3
$FeSO_4 \cdot 7H_2O$	25
$CaCl_2$	13.9
EDTA	100
$H_2C_2O_4$	40
Lotos-M	350
Mineralisation	*7035.47*

Methods of research

The experimental studies of the precipitates formed during the ozonation of simulated NPP wastewater solutions were carried out according to the following scheme (Fig. 1):

100 cm^3 of the simulated NPP wastewater solution was poured into a column. Then it was heated to the optimum temperature for organic component destruction — 60 °C and ozonated for 2 hours. Ozone was obtained in the ozone generator "Crozon-2001" OZP-6Y with a capacity of 2.5 g of O_3 per hour. The ozone-air mixture was fed into a 3.5 cm diameter and 31 cm high column from the bottom through the dispersant with an air flow rate of 1.2 m^3/h, as it is described in patent [15].

After ozonation, the test solutions were poured into conical flasks, where they were spontaneously cooled to room temperature.

The final pH value of the solution was determined using the pH meter pH-160 MI. The residual activity of ^{137}Cs was determined by γ-spectrometer SPE "OPYT" "ATOLL-1M" (measurement error ±20%). The newly formed precipitates were analysed by SEM/EDS, DTA and X-ray phase analysis.

Since the studied process is heterogeneous, the experiments were performed using inert granular loading, which increases the efficiency of the wastewater organic components destruction by increasing the contact surface of the phases of the analysed liquid and ozone-air mixture, and also improves mixing in the system. The amount of the organic substance in the solutions was determined by the dichromate chemical oxygen demand (COD) method. The maximum degree of the ozone destruction of the organic components in the simulated LRW solution was 67%.

Scanning electronic microscopy (SEM) and energy dispersion spectra (EDS). The analysis of the precipitates was performed using a scanning electron microscope JSM-6700F, equipped with an energy dispersion system for microanalysis JED-2300 (JEOL, Japan). SEM images and the chemical composition of the samples were obtained at an accelerating voltage of 15 kV, probe current of $6 \cdot 10^{-10}$ A and a probe diameter of 1 to 2 μm. Pure metals, minerals, oxides, and fluorides were used as standards.

X-ray phase analysis (X-ray diffractography). Phase composition of the precipitates was determined by the powder radiography method (X-ray phase analysis) using DRON-3 diffractometer with a copper anode radiation (CuKα). The scanning step was 0.05-0.1°, exposure — 4 seconds, 2θ diffraction angles — from 15 to 90°. Patterns were collected at standard temperature. The analysis of mineral composition was performed according to the ASTM file [26].

Results and discussion. SEM/EDS. A SEM image of the precipitate (Fig. 2, *a*, *b*) shows fine 20-30 nm spherical particles, probably metal oxides, associated in dense micro-sized aggre-
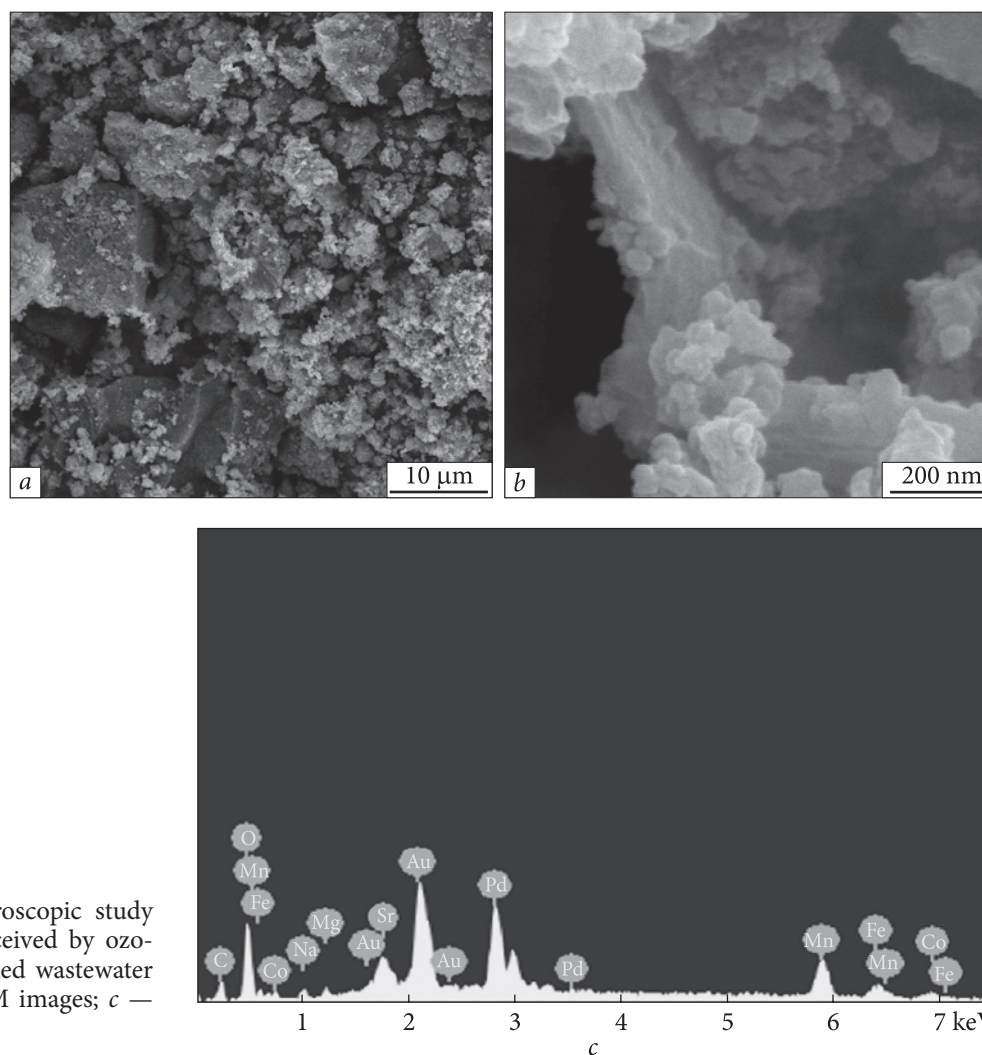
Fig. 2. Electron-microscopic study of the precipitate received by ozonation of the simulated wastewater solution: *a, b* — SEM images; *c* — EDS

gates and their associates of different configurations, usually with clear contours, and size ranging from 100 to 250 nm. Plate-shaped structures belong to layered double hydroxides of mixed composition, in particular Fe-Co, and iron oxyhydroxides — goethite and lepidocrocite [8]. A possible mechanism of phase formation is co-precipitation of ions during the destruction of organic components dissolved in wastewater and polycondensation of the precipitate, accompanied by adsorption processes [20].

After ozonation, the precipitate contained Mn, Fe, Co and negligible quanteties of Sr, Na and K [19]. Variations in the elemental composition of the precipitate depending on the morphology of the sample components were insignificant. Based on the percentage content of the components (weight and atomic percents), the following sequence can be suggested: Mn > Fe > Co > Sr > > Na > K (Fig. 2, *c*; Table 2). This is consistent with the stability constants of Mn, Fe, Co chelate complexes with EDTA [23]. The presence of Na and K is explained by their occlusion from the simulated solution, while the reflexions of precious metals are the result of the sample preparation procedure — spraying of the sample surface with Au and Pd.

X-ray phase analysis. X-ray phase analysis showed (Fig. 3) that the precipitate formed during ozonation is in a multi-component mineralized state. The original sample of iron-bearing compounds contains nano-size particles and a significant amount of amorphous matter. The amorphous phase has a significant specific surface area of the newly precipitated hydroxide, which is determined by the size of the particles. The crystallized compounds are presented predominantly by lepidocrocite γ-FeOOH (JCPDS file N 08-0098) and goethite α-FeOOH (JCPDS file N 17-536) phases. The content of the mag-
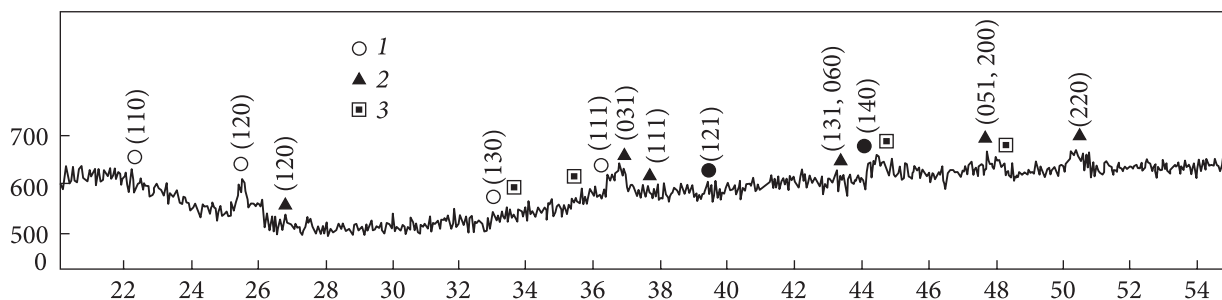
Fig. 3. Diffractogram of the original sample of the ferrum-manganese-bearing precipitate. The symbols (numbers) indicate the phases: *1* — goethite (α-FeOOH); *2* — lepidocrocite (γ-FeOOH); *3* — hydrated iron compounds, Fe(II)-Fe(III) layered double hydroxides

hemite phase γ-Fe_2O_3 (JCPDS file N 4-0755) is negligeable. The sample may contain several crystalline hydrates of basic salts of mixed composition, but their identification is complicated due to the low crystallinity of the sample and the overlapping of reflections from the planes (diffraction peaks) of several phases. In particular, the reflexes of iron (II) hydroxides (JCPDS file N 13-89) and iron (III) hydroxide (JCPDS file N 22-346) are observed. Maghemite and magnetite belong to ferromagnetics.

Manganese-bearing compounds are presented by manganese (IV) hydroxide (JCPDS file N 15-604) and manganese(II) carbonate (JCPDS file N 7-288), the diffraction patterns show reflections from planes (130), (400), (301) and planes (012), (104), (113), respectively. Weak single reflexes of hydrated manganese oxide $Mn_2O_3 \cdot H_2O$, manganese (II) oxide MnO (JCPDS file N 04-326) — planes (111), (200), (220), and double manganese oxide — gausmanite Mn_3O_4 are also identified.

Lyophilization of a precipitate sample at 160 °C for 2 hours contribute to the increase in the crystallinity of the precipitate and and partial dehydroxylation of the crystal lattice of iron and manganese (oxy)hydroxides (Fig. 4). The reflexes of the cubic crystal lattice present on the diffraction pattern can be attributed with equal probability to magnetite Fe_3O_4 (JCPDS file N 19-029) and gausmanite Mn_3O_4 (JCPDS file N 4-0731). The diffraction pattern also shows clear reflexes of manganese (II) carbonate $MnCO_3$ (JCPDS file N 7-288) and very intense reflexes of manganese (II) oxide MnO (110), (021), (201) (JCPDS file N 04-0326). The content of the amorphous component significantly decreases. The peaks of the residual phases of iron and manganese (oxy)hydroxides are overlapped by those of oxide phases.

The process of oxidative precipitation of the wastewater components by ozone is accompanied with the precipitate formation (secondary wastes), which necessitates its subsequent removing from the aqueous solutions. Magnetic separation can used for removing of the precipitate — effective and environmentally friendly method.

Analysis of the processes of groundwater and surface water purification from iron and manganese compounds when converting soluble Fe^{2+} and Mn^{2+} compounds into insoluble forms shows that parallel and competing complex processes of phase formation take place in the system [7, 10].

Formation of the goethite phase (FeOOH) from iron hydroxides occurs at high pH and

Table 2. **Elemental composition of the precipitates received by ozonation of the simulated wastewater solutions (according to EDS data)**

C	O	Na	Si	K	Ca	Mn	Fe	Co	Sr	Total
Weight %										
7.05	6.73	0.98	—	0.55	—	44.01	20.05	17.79	2.84	100
Atomic %										
22.87	16.38	1.66	—	0.88	—	31.20	13.98	11.76	1.26	100

Fig. 4. Diffractogram of ferrum-manganese-bearing precipitate after 2-hour heating at 160 °C. The symbols (numbers) indicate: *1* — cubic crystal lattice that characterizes magnetite and gausmanite; *2* — manganese (II) carbonate; *3* — manganese (II) oxide
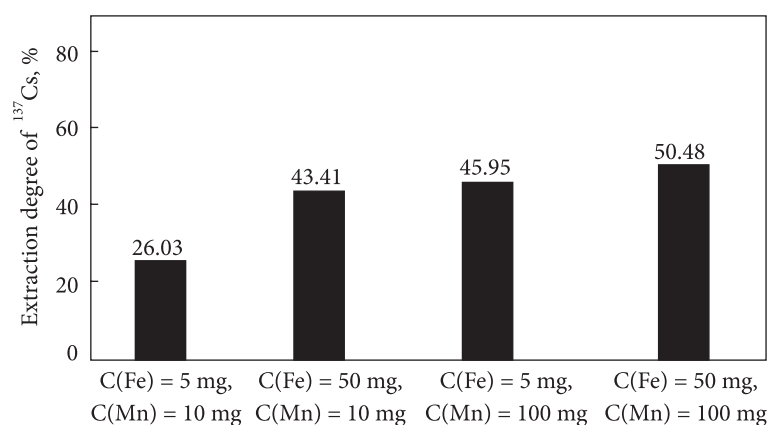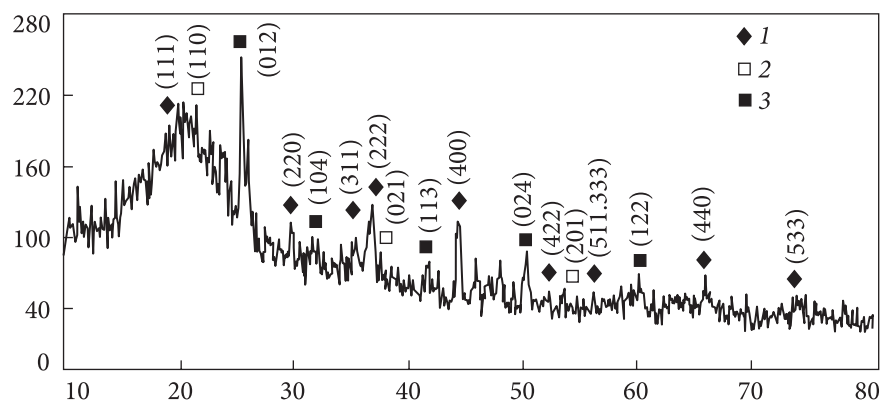

Fig. 5. The degree of ^{137}Cs extraction during ozonation, depending on the initial Fe^{2+} and Mn^{2+} concentrations

with the aging of amorphous hydroxide [16]. Precipitation at high temperatures and pH values ≤10 leads to the formation and aging of both α-FeOOH and anhydrous hematite α-Fe_2O_3 according to the reaction: $2FeOOH \rightarrow \alpha\text{-}Fe_2O_3 + H_2O$ [14]. During iron hydroxide gel formation, spherical particles are formed, which are later compacted and crystallized.

Lepidocrocite (γ-FeO(OH)) is formed by rapid oxidation of solutions containing iron(II) salts or suspension of $Fe(OH)_2$ with air oxygen [3]. Quite often, along with lepidocrocite, impurities of fine-crystalline goethite [3] or roentgen-amorphous iron(III) hydroxide gel are formed.

The theoretical composition of lepidocrocite is similar as that of goethite. However, compared to goethite, lepidocrocite contains more adsorbed water. Isomorphic substitution of iron for manganese up to 1.5 at.% is observed in γ-FeO(OH) [18].

Ferritization from aqueous solutions (pH ≥8) and formation of magnetite occurs from a liquid phase with the excess of oxygen [11]. The reaction of magnetite formation $Fe^{2+} + 2Fe^{3+} +$

$+ 8OH^- \leftrightarrow Fe_3O_4 + 4H_2O$ can be represented as the interaction of the ferric acid FeOOH salt, i.e. $Fe(FeOO)_2$, with water. The degree of the structuring and dispersion of hydromagnetite, as in the case of iron oxyhydroxides formation, depends in varying degrees on the alkalinity of the solution, the concentration of Fe(II), Fe(III) and OH ions, temperature and other factors. It should be stressed that ferritization, i.e. the formation of $Fe_2O_3 \cdot MeO$ from solutions containing metal ions, makes it possible to use this phenomenon to purify wastewater from heavy metal ions [9]. Magnetite is capable of isomorphic substitutions. Isomorphic substitution of iron for manganese up to 3.4 at.% was found [12].

With increasing of pH and aging, more crystallized iron phases are formed. They are characterized by smaller specific surface area and, consequently, a lower ability to adsorb microcomponents from the solution. Simultaneously, the increase in pH leads to coprecipitation of cations in the form of hydroxides and oxyhydroxides, which reduces the adsorption surface of ferritic precipitates. Increasing of the temperature during the precipitation of hydro-

xides and oxyhydroxides leads to accelerated hydrolysis, desorption of impurities from the precipitate surface, changes in the electric double layer structure, acceleration of the aging process and precipitate crystallization, etc.

In [17] it is shown that manganese-contaminated water purification results in formation of negatively charged manganese hydroxide $Mn(OH)_4$ which adsorbs positively charged manganese(II) ions and promotes sorption of negatively charged colloids $Fe(OH)_3$. When hydrolyzing, these ions react with the precipitate $Mn(OH)_4$ forming oxide Mn_2O_3 which is well oxidized and is a catalyst for the oxidation of iron, manganese and other heavy metal ions: $Mn(OH)_4 + Mn(OH)_2 \rightarrow Mn_2O_3 + 3H_2O$.

^{137}Cs sorption on precipitate during ozonation. Purification of man-made aqueous solutions from impurities of iron and manganese compounds is based on the sorption, coagulation and other surface processes that are achieved by application of predominantly oxidative methods and introduction of alkalizing reagents. The sorption processes are affected by many factors, e.g., the characteristics of the aquatic environment composition (pH, Eh, mineralization, forms of being of elements, etc.) and the sorbent (structure, specific surface area and porosity, etc.).

The amorphous phase of the insoluble iron and manganese compounds has a high specific surface area and, accordingly, the sorption capacity of precipitates towards radionuclides, in particular ^{137}Cs. Freshly prepared manganese precipitates have a specific surface area of about 300 m^2/g. The surface area of iron hydroxide precipitates is 300-400 m^2/g [7]. The positively charged Mn^{2+} cation facilitates sorption of the negatively charged colloids $Fe(OH)_3$.

As published in [6], at pH = 8-10, the freshly precipitated oxides and oxyhydroxides of Fe and Mn have a high sorption capacity towards cesium and strontium. The mechanism of cesium sorption is similar to the surface adsorption, which is almost independent of pH. Surface adsorption is accompanied by chemisorption with formation of ferrites. In the mixed iron-manganese oxides and oxyhydroxides, the increase in Mn:Fe ratio is followed by increase in Cs sorption. That is, in relation to cesium, the greatest selectivity is shown by the manganese dioxide, which due to surface adsorption con-

tains high amount of Cs, irrespective of the pH values. Iron hydroxides show increased sorption capacity for strontium in the alkaline environment with formation of ferrites.

On the other hand, sorbents based on manganese dioxide are selective mainly towards strontium isotopes due to steric factors: the size of the hydrated cations of cesium and strontium and the diameter of the macro- and micropores [5, 28].

Our studies of ^{137}Cs sorption on the precipitate during the wastewater ozonation have shown (Fig. 5) that increase in the Fe^{2+} and Mn^{2+} in the initial solution leads to a significant increase in the degree of ^{137}Cs extraction (up to 2 times). Thus, at the initial concentration of iron and manganese (5 and 10 mg/dm^3, respectively), the degree of Cs extraction was 26%. The 10-fold increase in the Fe^{2+} concentration, compared with the initial concentration up to 50 mg/dm^3, increased the degree of Cs extraction to 43%. The 10-fold increase in the Mn^{2+} concentration to 100 mg/dm^3 raised the degree of Cs extraction to almost 46%. Elevation of the concentration of both elements caused the increase of Cs extraction to 50.5%.

However, despite the increased sorption capacity of the precipitate formed by wastewater ozonation towards ^{134}Cs, ^{137}Cs radionuclides, it does not guarantee reliable immobilization of the adsorbed Cs radionuclides during the storage period. To increase the efficiency of wastewater decontamination, the conditions for simultaneous oxidative decomposition of the organic compounds by ozone and sorption of the basic dose-forming radionuclides on natural sorbents should be developed.

Conclusions. Scanning electron microscope image and energy dispersive spectra of the precipitates formed during ozonation of the simulated NPP wastewater solution (total mineralization 7 g/dm^3; pH = 11.5; T = 60°C; t = 2 h) showed the presence of finely dispersed 20-30 nm spherical particles, probably metal oxides, which are associated in solid microsized aggregates and their associates of different configuration. According to the elemental analysis, the main elements contained in the precipitates are Mn, Fe and Co, the concentration of Sr and Na is insignificant. According to the X-ray phase analysis data, the precipitate formed during

66

ISSN 2519-2396. Mineral. Journ. (Ukraine). 2022. 44, No. 2

ozonation of the simulated NPP wastewater solution is in a mineral-like form and contains, along with the amorphous phase, layered double Fe(II)-Fe(III) hydroxides of mixed composition, including Fe-Co and iron oxyhydroxides — goethite and lepidocrocitis. The manganese-containing compounds are presented by manganese (IV) hydroxide and manganese (II) carbonate, with admixtures of hydrated manganese oxide $Mn_2O_3 \cdot H_2O$, manganese (II) oxide MnO and double manganese oxide Mn_3O_4 — gaussmanite.

It is shown that the aging or heat treatment of the precipitates formed in the process of ozonation at 160 °C for 2 hours increases the degree of crystallinity of the precipitate and partially dehydroxylate the crystal lattice of iron and manganese (oxy)hydroxides.

During the ozonation of the simulated wastewater solutions that contain organic components, the processes of co-precipitation and adsorption of radionuclides proceed. With the 10-fold increase in the concentration of Fe^{2+} and Mn^{2+} ions, the concentration of ^{137}Cs in the solutions decreases by 26%, to 50.5%. To increase the efficiency of wastewater decontamination, a methodology for simultaneous oxidative decomposition of the organic compounds by ozone and sorption on the natural sorbents should be developed.

REFERENCES

1. Andronov, O.B. (2015), *Problemy bezpeky atomnykh elektrostantsiy i Chornobylia*, Vol. 24, Kyiv, UA, pp. 32-41 [in Russian].
2. Babenkov, E.D. (1974), *Ochistka vody koahuliantami*, Nauka, Moscow, RU, 356 p. [in Russian].
3. Petrovskaia, N.V. (ed.) (1975), *Gipergennye okisly zheleza v geologicheskih processah,* Nauka, Moscow, RU, 207 p. [in Russian].
4. Zhabrova, H.M. and Ehorov, E.V. (1961), *Uspekhi khymii,* Vol. 30, Iss. 6, pp. 764-776 [in Russian].
5. Karaseva, O.N., Ivanova, L.I. and Lakshtanov, L.Z. (2019), *Geochemistry*, Vol. 64, No. 10, Moscow, RU, pp. 1091-1104 [in Russian]. https://doi.org/10.31857/S0016-752564101091-1104
6. Kuznetsov, V.A. and Heneralova, V.A. (2000), *Radiokhimiia,* Vol. 42, No. 2, pp. 154-157 [in Russian].
7. Kuznetsov, Yu.V., Shchebetkovskiy, V.Ya. and Trusov, A.H. (1974), *Osnovy ochistki vody ot radioaktivnykh zahriazneniy*, Atomizdat, Moscow, RU, 232 p. [in Russian].
8. Lavrynenko, O.M. (2016), *Nano Studies*, No. 13, pp. 93-116 [in Russian].
9. Melikhov, I.V. and Merkulova, M.S. (1975), *Sokristallizatsiia*, Chemistry press, Moscow, RU, 280 p. [in Russian].
10. Neimark, Y.E. (1982), *Sinteticheskie mineralnye adsorbenty i nositeli katalizatorov*, Nauk. dumka, Kyiv, UA, 216 p. [in Russian].
11. Nikoladze, H.I. (1978), *Obezzhelezivanie prirodnykh i oborotnykh vod*, Stroiyzdat press, Moscow, RU, 160 p. [in Russian].
12. Povarennykh, A.S. (1966), *Kristallokhimicheskaia klassifikatsiia mineralnykh vidov*, Nauk. dumka, Kyiv, UA, 547 p. [in Russian].
13. (2016) *Povodzhennia z radioaktyvnymy vidkhodamy pry ekspluatatsii AES DP "NAEK "Enerhoatom". Zvit*, Kyiv, UA, 2016, 137 p. URL: https://www.sunpp.mk.ua/sites/default/files/documents/naek_zvit_rav_2016.pdf (Last accessed: 04.02.2022) [in Ukrainian].
14. Raspopov, Yu.H. (1982), in *Issledovaniia v oblasti tekhnolohii dvuokisi titana i zhelezosoderzhashchikh pihmentov*, Moscow, RU, pp. 87-93 [in Russian].
15. (2014) Пат. UA 88709 U. *Ustanovka dlia ochyshchennia vody vid orhanichnykh spoluk,* in Pliatsuk, L.D. and Roi, I.O., Published 25.03.2014, Bull. No. 6 [in Ukrainian].
16. Chalyi, V.P. (1972), *Hidrookisi metallov (zakonomernosti obrazovaniia, sostav, struktura i svoistva)*, Nauk. dumka, Kyiv, UA, 158 p. [in Russian].
17. Charnyi, D.V. and Matseliuk, Ye.M. (2019), *VI Int. sci.-pract. conf. "Chysta voda. Fundamentalni, prykladni ta promyslovi aspekty", 14-15 Novem. 2019,* Kyiv, UA, pp. 211-213 [in Ukrainian].
18. Shabalin, B.G. and Lavrynenko, O.M. (2020), *Yaderna enerhetyka ta dovkillia*, No. 3(18), Kyiv, UA, pp. 66-89 [in Ukrainian]. https://doi.org/10.31717/2311-8253.20.3.8
19. Shabalin, B.G., Lavrynenko, O.M., Yaroshenko, K.K., Vember, V.V. and Buhera, S.P. (2021), *XXII Int. sc.-pract. conf. "Ecology. Human. Sociaty",* Kyiv, UA, pp. 272-276 [in Ukrainian].
20. Yaroshenko, K.K., Shabalin, B.G. and Bondarenko, G.M. (2020), *Yaderna enerhetyka ta dovkillia,* No. 4(19), Kyiv, UA, pp. 32-39 [in Ukrainian]. https://doi.org/10.31717/2311-8253.20.4.4
21. Babuponnusami, A. and Muthukumar, K. (2014), *Environ. Chem. Eng.,* Vol. 2, pp. 557-572. https://doi.org/10.1016/j.jece.2013.10.011
22. (2003) *Combined methods for liquid radioactive waste treatment. Final report of a coordinated research project 1997-2001* IAEA-TECDOC-1336, pp. 121-136.

23. Martell, A.E. and Smith, R.M. (1974), Critical Stability Constants. *Plenum Press,* Vol. 3, New York, USA, 496 p.

24. (2014) *Mobile processing systems for radioactive waste management. Series No. NW-T-1.8,* Int. Atomic Energy Agency, Vienna, AT, 119 p.

25. Munter, R. (2001), *Proc. Estonian Acad. Sci. Chem.,* Vol. 50, No. 2, pp. 59-80.

26. (2003) *Powder diffraction file 2003*, PDF-2, Database. URL: https://www.icdd.com/pdf-2 (Last accessed: 04.02.2022).

27. Sam, A., Sam, W., Wooyong, U., Claire, L., Corkhill, N. and Corkhill, C.H. (2021), *Materials Degradation,* No. 5 (50). https://doi.org/10.1038/s41529-021-00192-3

28. Valsala, T.P., Joseph Annie, Sonar, N.L., Sonavane, M.S., Shah, J.G., Raj Kanwar and Venugopal, V. (2010), *J. Nuclear Mater.,* Vol. 404 (2), pp. 138-143. https://doi.org/10.1016/j.jnucmat.2010.07.017

Б.Г. Шабалін, д-р геол. наук, зав. відділу
E-mail: b_shabalin@ukr.net; https://orcid.org/0000-0002-6425-5999
К.К. Ярошенко, канд. техн. наук, наук. співроб.
E-mail: igns.yaroshenko@gmail.com; https://orcid.org/0000-0002-7180-4642
О.М. Лавриненко, д-р хім. наук, пров. наук. співроб.
E-mail: alena.lavrynenko@gmail.com; https://orcid.org/0000-0002-5271-2048
Н.Б. Міцюк, мол. наук. співроб.
E-mail: nmitsiuk@gmail.com; https://orcid.org/0000-0003-3875-007X
Державна установа "Інститут геохімії навколишнього середовища
Національної академії наук України"
03142, м. Київ, Україна, пр-т Акад. Палладіна, 34-а

МІНЕРАЛЬНИЙ СКЛАД ТА СОРБЦІЙНА ЗДАТНІСТЬ ЩОДО [137]Cs ОСАДІВ,
УТВОРЕНИХ В ПРОЦЕСІ ОЗОНУВАННЯ ТРАПНИХ ВОД АТОМНИХ ЕЛЕКТРОСТАНЦІЙ

Присвячено визначенню особливостей мінерального складу та сорбційних властивостей щодо [137]Cs осадів, утворених у процесі озонування модельних трапних вод атомних електричних станцій (загальна мінералізація 7 г/дм^3; pH = 11,5; T = 60 °С; t = 2 год). У досліджуваному осаді виявлено наявність тонкодисперсних частинок сферичної форми розмірами 20—30 нм, які асоційовані у щільні мікророзмірні агрегати та їхні асоціати різної конфігурації. Елементний склад осадів представлений Mn, Fe, Co з незначним вмістом Sr, Na і K. Осад перебуває в мінералізованому стані та містить з аморфною фазою шаруваті подвійні гідроксиди Fe(II)-Fe(III) змішаного складу, зокрема Fe-Co та оксигідроксиди феруму — гетит і лепідокрокіт. Мангановмісні сполуки представлені гідроксидом мангану(IV) та карбонатом мангану(II), з домішками гідратованого оксиду мангану $Mn_2O_3 \cdot H_2O$, оксиду мангану(II) MnO і подвійного оксиду мангану — гаусманіту Mn_3O_4. Ліофілізація осадів за температури 160 °С впродовж 2 год сприяє підвищенню ступеня їхньої кристалічності та частковому дегідроксилюванню кристалічної ґратки оксигідроксидів феруму та мангану. Під час озонування трапних вод відбуваються процеси деструкції органічних компонентів, сумісного осадження та адсорбції радіонуклідів. Визначено, що за збільшення концентрації катіонів Fe^{2+}, Mn^{2+} у 10 разів (до 50 та 100 мг/дм^3 відповідно) у вихідному розчині, концентрація [137]Cs у розчині зменшується на 50,5 %.

Ключові слова: трапні води АЕС, озонування, осади, хімічний і мінеральний склад, сорбція, цезій.